

Achieving tailorable magneto-caloric effect in the Gd-Co binary amorphous alloys

Cite as: AIP Advances 6, 035302 (2016); <https://doi.org/10.1063/1.4943506>

Submitted: 12 December 2015 . Accepted: 25 February 2016 . Published Online: 03 March 2016

C. Wu, D. Ding, L. Xia, and K. C. Chan



View Online



Export Citation



CrossMark

ARTICLES YOU MAY BE INTERESTED IN

[Magneto-caloric effect of a Gd₅₀Co₅₀ amorphous alloy near the freezing point of water](#)

AIP Advances 5, 097122 (2015); <https://doi.org/10.1063/1.4930832>

[Magnetocaloric effect in high Gd content Gd-Fe-Al based amorphous/nanocrystalline systems with enhanced Curie temperature and refrigeration capacity](#)

AIP Advances 6, 035220 (2016); <https://doi.org/10.1063/1.4945407>

[Large magnetic entropy change and adiabatic temperature rise of a Gd₅₅Al₂₀Co₂₀Ni₅ bulk metallic glass](#)

Journal of Applied Physics 115, 223904 (2014); <https://doi.org/10.1063/1.4882735>

AVS Quantum Science

Co-Published by



RECEIVE THE LATEST UPDATES



Achieving tailorable magneto-caloric effect in the Gd-Co binary amorphous alloys

C. Wu,^{1,2} D. Ding,² L. Xia,^{1,2} and K. C. Chan^{1,a}

¹Department of Industrial and Systems Engineering, The Hong Kong Polytechnic University, Hung Hom, Hong Kong

²Laboratory for Microstructure, Institute of Materials, Shanghai University, Shanghai 200072, China

(Received 12 December 2015; accepted 25 February 2016; published online 3 March 2016)

Tailorable magnetic properties and magneto-caloric effect were achieved in the Gd-Co binary amorphous alloys. It was found that the Curie temperature (T_c) of the $\text{Gd}_x\text{Co}_{100-x}$ ($x=50, 53, 56, 58, 60$) metallic glasses can be tuned by changing the concentration of Gd as $T_c = 708.8 - 8.83x$, and the mechanism involved was investigated. On the other hand, a linear correlation between the peak value of magnetic entropy change ($-\Delta S_m^{\text{peak}}$) and $T_c^{-2/3}$ is found in the amorphous alloys with a linear correlation coefficients of above 0.992. Therefore, the $-\Delta S_m^{\text{peak}}$ of the Gd-Co binary amorphous alloys under different magnetic fields can be easily tailored by adjusting the composition of the alloy. © 2016 Author(s). All article content, except where otherwise noted, is licensed under a Creative Commons Attribution (CC BY) license (<http://creativecommons.org/licenses/by/4.0/>). [<http://dx.doi.org/10.1063/1.4943506>]

Magnetic refrigeration (MR) based on the magneto-caloric effect (MCE) shows several advantages superior to the traditional vapor-compression refrigeration such as: i) the using of solid working substance, which does not produce high level of greenhouse gases; ii) the saving of energy cost as much as 30%; iii) low noise; iv) high reliability; v) long service life and so on.¹⁻³ It is well known that a practical magnetic refrigerant material, which is critical to the magnetic refrigerators, should exhibit excellent MCE, good mechanical properties, high corrosion resistance, low energy loss due to large electric resistance and nearly zero magnetic hysteresis. The unique properties of metallic glasses make the materials prospective candidates for magnetic refrigerant.⁴⁻²²

Metallic glasses undergo a second order magnetic transition and exhibit a broadened magnetic entropy change peak.⁸⁻²² Therefore, although the peak values of magnetic entropy change ($-\Delta S_m^{\text{peak}}$) for the metallic glasses are not as high as some of the crystalline alloys, the amorphous alloys still have evoked intensive interests because their refrigeration capacity (RC) are usually several times higher than that of the crystalline alloys. Our recent results have shown that the RC can reach an ultra-high value of above $800 \text{ J}\cdot\text{kg}^{-1}$ under 5 T, accompanied with a relatively high $-\Delta S_m^{\text{peak}}$ value of nearly $10 \text{ J}\cdot\text{kg}^{-1}\cdot\text{K}^{-1}$ under 5 T in some of the Gd-based metallic glasses.¹⁹⁻²² Besides, as the essential requirement for industrial application of the magneto-caloric materials, the metallic glasses can be fabricated in a wide compositional range and thus the tailorable magnetic properties can be easily achieved in metallic glasses by adjusting the composition within the compositional range of glass forming alloys. However, the mechanism for the tailorable properties of the metallic glasses, such as the compositional dependence of the Curie temperature (T_c), has not been studied systematically.

In the present work, we employed a simple Gd-Co binary alloy system for the investigation of the compositional dependence of magnetic properties of metallic glasses and the mechanism involved. Based on our preliminary work on the glass forming ability of the Gd-Co binary alloys, we selected $\text{Gd}_x\text{Co}_{100-x}$ ($x=50, 53, 56, 58, 60$) amorphous ribbons for the investigation. The field dependence of $-\Delta S_m^{\text{peak}}$ was constructed for the investigation of magneto-caloric behavior of the

^aCorresponding author: Email: kc.chan@polyu.edu.hk

metallic glasses. The relationships between Gd concentration and T_c , T_c and $-\Delta S_m^{peak}$ were also constructed for revealing the mechanism of tailorable MCE of the Gd-Co amorphous alloys.

Ingots of Gd-Co alloys with nominal compositions Gd_xCo_{100-x} ($x=45, 50, 53, 56, 58, 60, 61$) were prepared by arc-melting a mixture of the Gd and Co elements, respectively. The purity both the Gd and Co elements is above 99.9% (at%). The ingots were remelted for at least four times under a titanium-gettered argon atmosphere to ensure the homogeneity of the mother alloys. As-spun ribbons are produced by melt-spinning in a high-purified argon atmosphere using a single copper wheel with a surface speed of 30 m/s single-roller. The structure of the ribbons was characterized by X-ray diffraction (XRD) on a Rigaku D\max-2550 diffractometer using $Cu K_\alpha$ radiation. A Quantum Design Physical Properties Measurement System (PPMS 6000) was used to measure the magnetic properties of the amorphous ribbons. The temperature dependence of the magnetization ($M-T$) curves was measured under a field of 0.03 T in the cooling process. The hysteresis loops were measured at the temperature well below the Curie temperature under a field of 2 T. The isothermal magnetization curves ($M-H$) of the amorphous ribbons were measured at selected temperatures under a field of 5 T. All the data obtained by PPMS were corrected by high purity Ni.

Our preliminary results have demonstrated that some of the Gd-Co binary amorphous alloys can be fabricated in the shape of ribbons under a high cooling rate.²³ Figure 1 shows the XRD patterns of Gd_xCo_{100-x} ($x=45, 50, 53, 56, 58, 60, 61$) ribbons obtained at a wheel surface speed of 30 m/s. $Gd_{50}Co_{50}$, $Gd_{53}Co_{47}$, $Gd_{56}Co_{44}$, $Gd_{58}Co_{42}$ and $Gd_{60}Co_{40}$ ribbons exhibit typical amorphous characteristics of broadened diffraction maxima in the XRD patterns, while $Gd_{45}Co_{55}$ and $Gd_{61}Co_{39}$ are partially crystallized. The $Gd_{50}Co_{50}$, $Gd_{53}Co_{47}$, $Gd_{56}Co_{44}$, $Gd_{58}Co_{42}$ and $Gd_{60}Co_{40}$ amorphous ribbons are therefore employed for the further investigation on magnetic properties and magneto-caloric effect of Gd-Co amorphous alloys.

Figure 2(a) shows the $M-T$ curves of the Gd_xCo_{100-x} ($x=50, 53, 56, 58, 60$) amorphous ribbons measured under a magnetic field of 0.03 T. The Curie temperature of the amorphous ribbons obtained from the derivative of their $M-T$ curves respectively is about 267 K for $Gd_{50}Co_{50}$, 241 K for $Gd_{53}Co_{47}$, 216 K for $Gd_{56}Co_{44}$, 196 K for $Gd_{58}Co_{42}$ and 179 K for $Gd_{60}Co_{40}$, respectively. As shown in Fig. 2(b), T_c decreases monotonically with the increasing Gd concentration, indicating that the Curie temperature of the Gd-Co amorphous alloys can be tuned by changing the concentration of Gd or Co on the binary alloys. The compositional dependence of T_c for the Gd_xCo_{100-x} ($x=50, 53, 56, 58, 60$) amorphous ribbons follows a $T_c=708.8-8.83x$ relationship by linear fitting.

It is known that there are three kinds of exchange interaction in the Gd-Co binary alloys, the strong interaction between Co and Co atoms, and the indirect interactions between Gd-Gd atoms and Gd-Co atoms. The ordering temperature, namely, the Curie temperature of the Gd-Co amorphous alloys is mainly determined by the strong interaction between Co-Co atoms, which is closely related to the local environment of Co atoms.^{24,25} The increase of Gd concentration, however, will

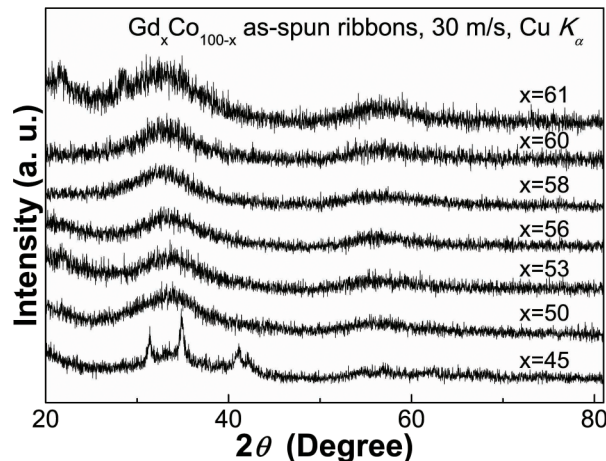


FIG. 1. XRD patterns of the Gd_xCo_{100-x} ($x=45, 50, 53, 56, 58, 60, 61$) as-spun ribbons.

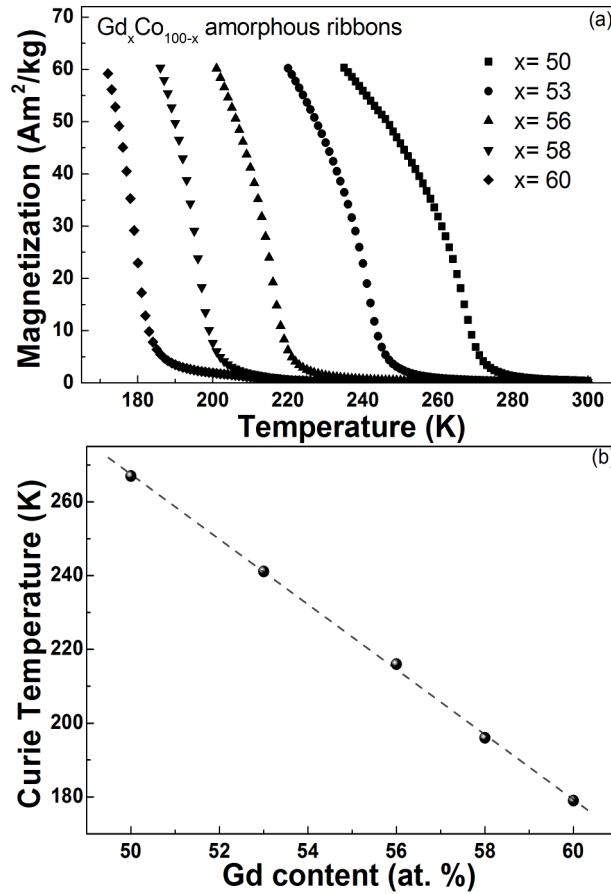


FIG. 2. (a) M - T curves of the Gd_xCo_{100-x} ($x=50, 53, 56, 58, 60$) amorphous ribbons; (b) the relationship between the T_c and the Gd concentration x .

simultaneously reduce the amount of Co atoms, which means enlarge the distance between Co atoms and thus diminish the Co-Co interaction of the amorphous alloys. On the other hand, the interactions involving Gd, that is, the indirect interactions between Gd-Gd and Gd-Co, play a more important role in determining the magnetic behavior of the amorphous alloys. The increase of Gd concentration will enhance the Gd-Co indirect interaction, which may reduce the density of the Fermi surface states and lead to the suppression of Co-Co interaction.²⁵ As a result, Gd-Co alloys containing less Co show lower Curie temperature, while most of the rare earth (R)-transition metal (M) permanent magnets such as the Sm_2Co_{17} exhibit much higher T_c .²⁶

The linear relationship between the alloy composition and T_c indicates the tailorable magneto-caloric effect of the Gd-Co amorphous alloys according to relationship between $-\Delta S_m^{peak}$ and $T_c^{-2/3}$ proposed recently by Belo *et al.* recently as follows:²⁷

$$-\Delta S_m^{peak} = \frac{1}{2C} \left(\frac{C^2}{K} \right)^{\frac{2}{3}} \left(\frac{H}{T_c} \right)^{\frac{2}{3}} + \dots$$

where $C = NJ(J+1)g^2\mu_B^2/(3k_B)$ and $K = (2J^2 + 2J + 1)/[10J(J+1)k_B N]$, N is the density of the magnetic atoms, g is the Lande factor, μ_B is the Bohr magneton, k_B is the Boltzmann constant, J is the total spin number, and H is the applied magnetic field. For the binary Gd-Co amorphous alloys, the parameters N , μ_B and k_B are constants. J for the Gd_xCo_{100-x} ($x = 50, 53, 56, 58, 60$) amorphous alloys can be expressed as $J = [7x/2 + 3(100-x)/2]/100 = 1.5 + 0.02x$. g of the amorphous alloys can be expressed as $g = [2x + 4/3(100-x)]/100 = 4/3 + x/150$. T_c of the Gd_xCo_{100-x} amorphous alloys, as mentioned above, is about $708.8 - 8.83x$. As a result, the $-\Delta S_m^{peak}$ of the Gd_xCo_{100-x} glassy ribbons under a specific magnetic field can be determined by the composition of the alloys.

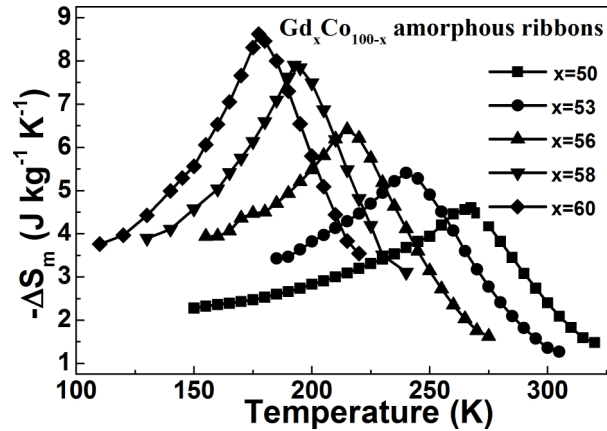


FIG. 3. The $(-\Delta S_m)$ - T curves of the Gd_xCo_{100-x} ($x=50, 53, 56, 58, 60$) amorphous ribbons under a field of 5 T.

The magnetic entropy change (ΔS_m) of the Gd_xCo_{100-x} ($x=50, 53, 56, 58, 60$) amorphous alloys can be derived from the isothermal M - H curves according to the Maxwell equation.²⁸ Figure 3 shows the $(-\Delta S_m)$ - T curves of Gd_xCo_{100-x} ($x=50, 53, 56, 58, 60$) amorphous alloys under a field of 5 T. Each sample shows a broadened $-\Delta S_m$ peak, which is the typical characteristics of amorphous alloys undergoing a second order magnetic phase transition.^{1,29} $-\Delta S_m^{peak}$ of the amorphous $Gd_{50}Co_{50}$, $Gd_{53}Co_{47}$, $Gd_{56}Co_{44}$, $Gd_{58}Co_{42}$ and $Gd_{60}Co_{40}$ ribbons under a field of 5T are $4.60 \text{ J}\cdot\text{kg}^{-1}\text{K}^{-1}$, $5.41 \text{ J}\cdot\text{kg}^{-1}\text{K}^{-1}$, $6.41 \text{ J}\cdot\text{kg}^{-1}\text{K}^{-1}$, $7.90 \text{ J}\cdot\text{kg}^{-1}\text{K}^{-1}$ and $8.62 \text{ J}\cdot\text{kg}^{-1}\text{K}^{-1}$, respectively. The value of $-\Delta S_m^{peak}$ for the amorphous ribbons increase obviously with the increasing concentration of Gd, which is most likely due to the enhanced Gd-Co indirect interaction with the increasing Gd concentration. And thus the amorphous $Gd_{60}Co_{40}$ alloy containing only 60% (at. %) Gd exhibits a high value of $-\Delta S_m^{peak}$ up to about 88% as high as pure Gd.

It is known that the field dependence of $-\Delta S_m$ for an amorphous alloy undergoing a second-order magnetic phase transition can be expressed as $-\Delta S_m \propto H^n$.^{20-22,30-32} In general, as proposed by Franco according to the Arrott-Noakes equation,³⁰ the n value changes with temperature as follows: $n=1$ at the temperature well below T_c , $n=2$ at the temperature much higher than T_c , and $n \approx 0.72$ at the temperature near T_c . Therefore, the investigation on the field dependence of $-\Delta S_m^{peak}$ for the Gd_xCo_{100-x} ($x=50, 53, 56, 58, 60$) as-spun ribbons will be helpful for the identification of amorphous characteristics of the ribbons. $-\Delta S_m^{peak}$ of Gd-Co amorphous alloys under different magnetic fields obtained from the $(-\Delta S_m)$ - T curves are listed in Table I. Thus the $-\Delta S_m^{peak}$ vs H plots of the Gd_xCo_{100-x} ($x=50, 53, 56, 58, 60$) amorphous alloys can be constructed accordingly, as shown in Fig. 4. From the $-\Delta S_m^{peak} \propto H^n$ fittings for each amorphous alloy, we can obtain the n value of 0.75 for $Gd_{50}Co_{50}$, 0.737 for $Gd_{53}Co_{47}$, 0.727 for $Gd_{56}Co_{44}$, 0.7 for $Gd_{58}Co_{42}$ and 0.686 for $Gd_{60}Co_{40}$ ribbons, respectively. The n values of the Gd_xCo_{100-x} ($x=50, 53, 56, 58, 60$) amorphous alloys are similar to those of other amorphous alloys, indicating the typical magneto-caloric behaviors of amorphous alloys.

Figure 5 shows the $-\Delta S_m^{peak}$ vs $T_c^{-2/3}$ (or $(708.8-8.83x)^{-2/3}$) plots of the Gd_xCo_{100-x} ($x=50, 53, 56, 58, 60$) amorphous alloys under the magnetic field ranging from 1 T to 5 T. A linear relationship

TABLE I. $-\Delta S_m^{peak}$ of Gd-Co amorphous alloys under different magnetic fields.

$-\Delta S_m^{peak}$ ($\text{J}\cdot\text{kg}^{-1}\text{K}^{-1}$)	1T	2T	3T	4T	5T
$Gd_{50}Co_{50}$	1.38	2.36	3.16	3.92	4.6
$Gd_{53}Co_{47}$	1.66	2.78	3.74	4.61	5.41
$Gd_{56}Co_{44}$	1.99	3.34	4.47	5.48	6.41
$Gd_{58}Co_{42}$	2.56	4.22	5.58	6.8	7.9
$Gd_{60}Co_{40}$	2.84	4.74	6.1	7.42	8.62

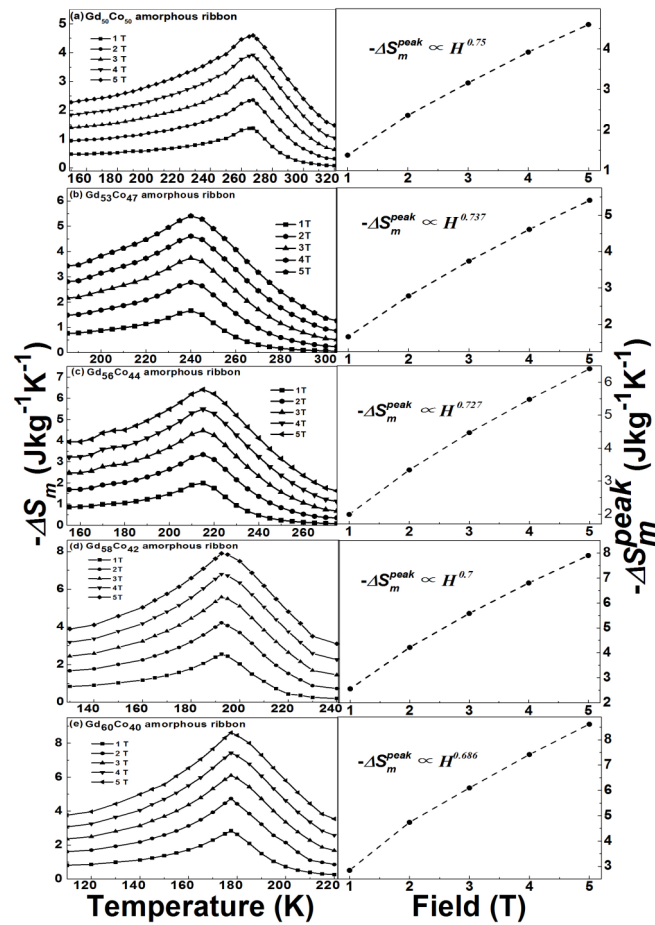


FIG. 4. The temperature dependence of $-\Delta S_m$ and the field dependence of $-\Delta S_m^{peak}$ for the Gd_xCo_{100-x} amorphous ribbons under the magnetic fields ranging from 1 T to 5 T: (a) $Gd_{50}Co_{50}$, (b) $Gd_{53}Co_{47}$, (c) $Gd_{56}Co_{44}$, (d) $Gd_{58}Co_{42}$ and (e) $Gd_{60}Co_{40}$, respectively.

between $-\Delta S_m^{peak}$ and $T_c^{-2/3}$ (or $(708.8-8.83x)^{-2/3}$) is found in Gd-Co binary amorphous alloys and the linear correlation coefficients are above 0.992. Therefore, as predicted above, the $-\Delta S_m^{peak}$ of the Gd-Co binary amorphous alloys under different magnetic fields can be easily tailored by adjusting the composition of the alloy.

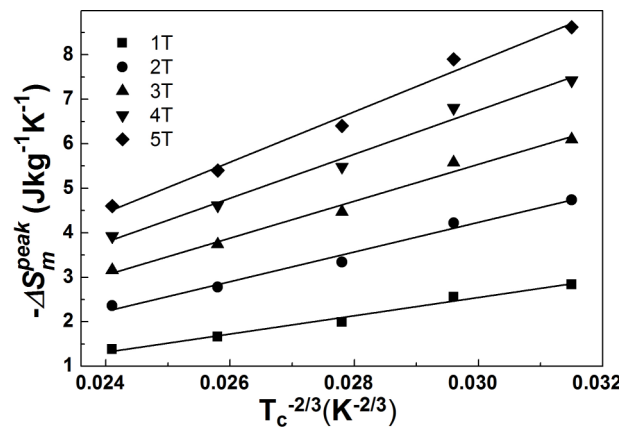


FIG. 5. The dependence of $-\Delta S_m^{peak}$ on $T_c^{-2/3}$ under the magnetic fields ranging from 1 T to 5 T.

In summary, we obtained tailorable magnetic properties and magneto-caloric effect in the Gd-Co binary amorphous alloys. The magnetic properties and magneto-caloric effects of $\text{Gd}_x\text{Co}_{100-x}$ ($x=50, 53, 56, 58, 60$) amorphous alloys fabricated in the shape of ribbons were investigated. It was found that T_c of the ribbons decreases monotonically with the increasing Gd concentration, which is supposed to be due to the suppression of Co-Co interaction with the increase of Gd concentration. The linear relationship between the alloy composition and T_c can be expressed as $T_c = 708.8 - 8.83x$, indicating the tailorable magneto-caloric effect of the Gd-Co amorphous alloys according to relationship between $-\Delta S_m^{\text{peak}}$ and $T_c^{-2/3}$ proposed by Belo *et al.* Experimental results have revealed a linear dependence of $-\Delta S_m^{\text{peak}}$ on $T_c^{-2/3}$ (or $(708.8 - 8.83x)^{-2/3}$) in the $\text{Gd}_x\text{Co}_{100-x}$ ($x=50, 53, 56, 58, 60$) amorphous alloys, justifying the tailorable $-\Delta S_m^{\text{peak}}$ by adjusting the composition of Gd-Co binary alloys.

The work described in this paper was mainly supported by the Research Grants Council of the Hong Kong Special Administrative Region, China (Project No. PolyU 511212).

- ¹ K. A. Gschneidner and V. K. Pecharsky, Jr., *Annu. Rev. Mater. Sci.* **30**, 387 (2000).
- ² E. Bruck, *J. Phys. D* **38**, R381 (2005).
- ³ K. A. Gschneidner, Jr., V. K. Pecharsky, and A. O. Tsokol, *Rep. Prog. Phys.* **68**, 1479 (2005).
- ⁴ A. Inoue, *Acta Mater.* **48**, 279 (2000).
- ⁵ W. L. Johnson, *JOM* **54**, 40 (2002).
- ⁶ W. H. Wang, C. Dong, and C. H. Shek, *Mater. Sci. Eng. R* **44**, 45 (2004).
- ⁷ A. Inoue and A. Takeuchi, *Acta Mater.* **59**, 2243 (2011).
- ⁸ M. Földeaki, A. Giguère, B. R. Gopal, R. Chahine, T. K. Bose, X. Y. Liu, and J. A. Barclay, *J. Magn. Magn. Mater.* **174**, 295 (1997).
- ⁹ M. Földeaki, R. Chahine, B. R. Gopal, T. K. Bose, X. Y. Liu, and J. A. Barclay, *J. Appl. Phys.* **83**, 2727 (1998).
- ¹⁰ A. Atlay, H. Gencer, and V. S. Kolat, *J. Non-Cryst. Solids* **351**, 2373 (2005).
- ¹¹ X. Y. Liu, J. A. Barclay, M. Földeaki, B. R. Gopal, R. Chahine, and T. K. Bose, *Adv. Cryog. Eng.* **42**, 431 (1996).
- ¹² N.S. Bingham, H. Wang, F. Qin, H.X. Peng, J.F. Sun, V. Franco, H. Srikanth, and M.H. Phan, *Appl. Phys. Lett.* **101**, 102407 (2012).
- ¹³ B. Schwarz, N. Mattern, Q. Luo, and J. Eckert, *J. Magn. Magn. Mater.* **324**, 1581 (2012).
- ¹⁴ F. X. Qin, N.S. Bingham, H. Wang, H.X. Peng, J.F. Sun, X. Franco, S.C. Yu, H. Srikanth, and M.H. Phan, *Acta Mater.* **61**, 1284 (2013).
- ¹⁵ V. Franco, J. M. Borrego, A. Conde, and S. Roth, *Appl. Phys. Lett.* **88**, 132509 (2006).
- ¹⁶ P. Alvarez-Alonso, J. L. Sánchez Llamazares, C. F. Sánchez-Valdés, M. L. Fdez-Gubieda, P. Gorria, and J. A. Blanco, *J. Appl. Phys.* **117**, 17A710 (2015).
- ¹⁷ V. Franco, C. F. Conde, A. Conde, and L. F. Kiss, *Appl. Phys. Lett.* **90**, 052509 (2007).
- ¹⁸ Q. Y. Dong, B. G. Shen, J. Chen, J. Shen, F. Wang, H. W. Zhang, and J. R. Sun, *J. Appl. Phys.* **105**, 053908 (2009).
- ¹⁹ L. Xia, C. Wu, S. H. Chen, and K. C. Chan, *AIP Advances*, **5**, 097122 (2015).
- ²⁰ L. Xia, M.B. Tang, K.C. Chan, and Y.D. Dong, *J. Appl. Phys.* **115**, 223904 (2014).
- ²¹ L. Xia, Q. Guan, D. Ding, M.B. Tang, and Y.D. Dong, *Appl. Phys. Lett.* **105**, 192402 (2014).
- ²² C. Wu, P. Yu, and L. Xia, *Journal of Non-Cryst. Solids* **422**, 23 (2015).
- ²³ Y. F. Ma, P. Yu, and L. Xia, *Materials and Design* **85**, 715 (2015).
- ²⁴ E. Belorizky, M. A. Fremy, J. P. Gavigan, D. Givord, and H. S. Li, *J. Appl. Phys.* **61**, 3971 (1987).
- ²⁵ J. H. Zhang, S. Liu, F. Gu, L. J. Yang, and M. Liu, *Acta Phys. Sin.* **55**, 2928 (2006).
- ²⁶ J. R. Jeffries, L. S. I. Veiga, G. Fabbris, D. Haskell, P. Huang, N. P. Butch, S. K. McCall, K. Holliday, Z. Jenei, Y. Xiao, and P. Chow, *Phys. Rev. B* **90**, 104408 (2014).
- ²⁷ J. H. Bloie, J. S. Amaral, A. M. Pereira, V. S. Amaral, and J. P. Araujo, *Appl. Phys. Lett.* **100**, 242407 (2012).
- ²⁸ T. Hashimoto, T. Numasawa, M. Shino, and T. Okada, *Cryogenics* **21**, 647 (1981).
- ²⁹ A. M. Tishin and Y. I. Spichkin, *Magnetocaloric Effect and its Applications* (Institute of Physics, Bristol, 2003).
- ³⁰ V. Franco, J. S. Blázquez, and A. Conde, *Appl. Phys. Lett.* **89**, 222512 (2006).
- ³¹ V. Franco, J. M. Borrego, C. F. Conde, A. Conde, M. Stoica, and S. Roth, *J. Appl. Phys.* **100**, 083903 (2006).
- ³² V. Franco, J. S. Blázquez, and A. Conde, *J. Appl. Phys.* **100**, 064307 (2006).